

Determination of thermodynamic functions and structural parameters of NpO₂⁺ lactate complexes

Maiwald, M. M.; Müller, K.; Heim, K.; Trumm, M.; Fröhlich, D. R.; Banik, N. L.; Rothe, J.;
Dardenne, K.; Skerencak-Frech, A.; Panak, P. J.;

Originally published:

September 2020

New Journal of Chemistry 44(2020)39, 17033-17046

DOI: <https://doi.org/10.1039/d0nj04291a>

Perma-Link to Publication Repository of HZDR:

<https://www.hzdr.de/publications/Publ-31033>

Release of the secondary publication
on the basis of the German Copyright Law § 38 Section 4.

Determination of thermodynamic functions and structural parameters of NpO_2^+ lactate complexes

M. M. Maiwald^{1*}, K. Müller³, K. Heim³, M. Trumm², D. R. Fröhlich¹, N. L. Banik⁴, J. Rothe², K. Dardenne², A. Skerencak-Frech², P. J. Panak^{1,2}

- 1) Ruprecht Karls Universität Heidelberg, Physikalisch-Chemisches Institut, Im Neuenheimer Feld 253, D-69120 Heidelberg, Germany
- 2) Karlsruher Institut für Technologie (KIT), Institut für Nukleare Entsorgung (INE), D-76344 Eggenstein-Leopoldshafen, Germany
- 3) Helmholtz-Zentrum Dresden-Rossendorf, Institut für Ressourcenökologie, Bautzner Landstraße 400, 01328 Dresden, Germany
- 4) Joint Research Center JRC - Karlsruhe, G.II.6 - Nuclear Safeguards and Forensics, European Commission, P.O.Box 2340, D-76125 Karlsruhe, Germany

* E-mail: m.maiwald@pci.uni-heidelberg.de

Abstract

The complexation of NpO_2^+ with lactate in aqueous solution is studied as a function of the total ligand concentration ($[\text{Lac}]_{\text{total}}$), ionic strength ($I_m = 0.5 - 4.0 \text{ mol kg}^{-1} \text{ Na}^+(\text{Cl}^-/\text{ClO}_4^-)$) and temperature ($T = 20 - 85 \text{ }^\circ\text{C}$) by Vis/NIR absorption spectroscopy. The formation of two NpO_2^+ lactate species with the stoichiometry $\text{NpO}_2(\text{Lac})_n^{1-n}$ ($n = 1, 2$) is observed at the studied experimental conditions. The temperature dependent conditional stability constants $\log \beta'_j(T)$ at different ionic strengths are calculated with the law of mass action. The conditional data are extrapolated to IUPAC reference state conditions ($I_m = 0$) with the specific ion interaction theory (SIT). With increasing temperature up to $85 \text{ }^\circ\text{C}$ $\log \beta^0_1(20 \text{ }^\circ\text{C}) = 1.92 \pm 0.14$ decreases by 0.12 and $\log \beta^0_2(20 \text{ }^\circ\text{C}) = 2.10 \pm 0.13$ decreases by 0.17. The thermodynamic stability constants correlate linearly with the reciprocal temperature according to the integrated Van't Hoff equation. Thus, linear regression analyses yield the standard reaction enthalpy $\Delta_r H^0$ and entropy $\Delta_r S^0$ for the complexation reactions. In addition, the sum of the SIT specific binary ion-ion interaction coefficients $\Delta \varepsilon_{j,k}(T)$ of the complexation reactions are determined by variation of the ionic strength.

Structural parameters of the formed complex species and the coordination mode of lactate towards the NpO_2^+ ion are investigated as a function of pH_c by extended x-ray absorption fine structure

spectroscopy (EXAFS) and attenuated total reflection Fourier-transform infrared spectroscopy (ATR-FT IR). The results show, that the coordination mode of lactate changes from end-on (coordination via only the COO⁻ group) to side-on (formation of chelate rings involving the OH-group) with increasing pH. The experiments are supported by quantum chemical calculations.

1 Introduction

Deep geological formations are considered for the final disposal of high-level nuclear waste. Suitable host rock formations discussed in several European countries (e.g. Belgium¹, France², Germany³ and Switzerland⁴) are rock salt, crystalline formations (e.g. granite) and clay rocks. Due to their long half-lives, the transuranium element plutonium (Pu) and the minor actinides (Np, Am) determine the long-term radiotoxicity of the nuclear waste. Therefore, the actinides are of particular interest for the safety case of a nuclear waste repository. In case of a release of radionuclides from the primary containments, a mechanistic understanding of the most relevant interactions (e.g. dissolution of the waste matrix and solubility of the radionuclides, sorption and complexation processes, etc.) of the radionuclides with the surrounding backfill material, the host rock, and the aquifer components is essential. In particular complexation reactions with naturally occurring inorganic and organic ligands in aqueous solution can significantly affect the mobility and migration of the radionuclides.

Depending on the repository design and host-rock characteristics increased temperatures are expected in the near-field of a nuclear waste repository e.g. up to 100 °C for clay rocks and up to 200 °C for salt rocks.⁵ Additionally, some clay repository sites exhibit high saline conditions, e.g. in Northern Germany the ionic strength of the pore water is above 3.5 mol L⁻¹.³ It was shown earlier that an increase of the temperature and the ionic strength may have a significant influence on complexation processes with different organic and inorganic components in natural aquatic systems affecting the retardation efficiency of the host rock.⁶ Low-molecular-weight organic compounds (LMWOC) like formate, acetate, propionate, and lactate make up large fractions of the dissolved organic matter in the pore waters of different clay formations (e.g. Callovo Oxfordian (Cox) and Opalinus Clay (OPA)).⁷⁻¹⁰ Among the LMWOC lactate is only present in concentrations up to [Lac⁻] = 17 μM but is of particular interest as it provides the possibility to coordinate to the metal ion in different coordination modes.^{9, 10} This contrasts to mono carboxylic ligands (e.g. acetate, propionate) as the lactate molecule can either coordinate *end-on* via the carboxyl function or *side-on* via both the COO⁻ group and the α-hydroxy group. The coordination mode of lactate might also be affected by the pH value. In addition, lactate can be used to study the effect of α-OH groups in organic compounds on the complex stability, thermodynamic behaviour and structure of An-LMWOC complexes.

Actinides in the pentavalent oxidation state are known to be highly soluble with low retention by mineral phases.¹¹⁻¹⁷ Within the series of the An(V) the Np(V) ion is the most stable in aqueous solution and is used as an analogue for the An(V) due to its excellent spectroscopic properties.

The present work focusses on the determination of thermodynamic data for the complexation of NpO_2^+ with lactate. Thermodynamic data on NpO_2^+ lactate complexes are scarce in the literature and no thermodynamic functions ($\Delta_r H^0$, $\Delta_r S^0$, $\Delta \varepsilon_{j,k}(T)$) are available. Different studies based on solvent extraction and spectrophotometry report different results concerning the speciation of the NpO_2^+ lactate complexes.¹⁸⁻²⁰ Depending on the experimental approach the formation of only $\text{NpO}_2(\text{Lac})$ or both $\text{NpO}_2(\text{Lac})$ and $\text{NpO}_2(\text{Lac})_2^-$ was observed. Also, the reported stability constants for $\text{NpO}_2(\text{Lac})$ differ significantly ($\log \beta'(25\text{ }^\circ\text{C}) = 1.1 - 1.8$, at $I_m(\text{NaClO}_4) = 1\text{ mol kg}^{-1}$).

Furthermore, structural investigations are of particular interest as no structural data of An(V)-lactate complexes are available in the literature describing the complexation of An(V) with α -hydroxy carboxylates on a molecular level.

In the present work the complexation of NpO_2^+ with lactate as a function of the ligand concentration, temperature and ionic strength is studied by Vis/NIR absorption spectroscopy. Structural characterization of the complexes is performed by extended x-ray absorption fine structure spectroscopy (EXAFS) and attenuated total reflection Fourier-transform infrared (ATR FT-IR) spectroscopy. The experimental data are supported by quantum chemical calculations.

2 Experimental

2.1 Sample Preparation

Caution! ²³⁷Np is an α -emitter and must be handled with care in laboratories appropriate for research involving transuranic elements. Health risks caused by radiation exposure or incorporation must be avoided. Higher concentrated Np solutions were handled in glove boxes.

The molal concentration scale ($\text{mol kg}^{-1}\text{ H}_2\text{O}^{-1}$, "m") was used for all solutions to avoid changes of the concentration caused by changes of the temperature or the ionic strength. All chemicals except for neptunium were reagent grade or higher and purchased from Merck Millipore. For sample preparation ultrapure water (Milli-Q academic, Millipore, $18.3\text{ M}\Omega\text{ cm}^{-1}$) was used.

Absorption spectroscopy: The total initial NpO_2^+ concentration of all samples used for absorption spectroscopy was adjusted to $2.5 \times 10^{-4}\text{ mol kg}^{-1}$ in $2.1 \times 10^{-5}\text{ mol kg}^{-1}\text{ HClO}_4$ by dilution of a $4.3 \times 10^{-2}\text{ mol kg}^{-1}\text{ }^{237}\text{NpO}_2^+$ stock solution ($[\text{HClO}_4]_{\text{stock}} = 2.9 \times 10^{-3}\text{ mol kg}^{-1}$). The preparation of the stock solution is described in the literature.²¹ The complexation of NpO_2^+ was studied as a function of $[\text{Lac}]_{\text{tot}}$ at three different ionic strengths ($I_m = 0.5, 2.0$ and $3.6\text{ mol kg}^{-1}\text{ Na}(\text{ClO}_4^-/\text{Lac}^-)$) and $T = 20\text{ }^\circ\text{C}$. The temperature dependence ($T = 20 - 85\text{ }^\circ\text{C}$) of the complexation reactions was determined as a function of $[\text{Lac}]_{\text{tot}}$ at

$I_m = 3.6 \text{ mol kg}^{-1} \text{ Na}(\text{ClO}_4^-/\text{Lac}^-)$. The ionic strength dependence of the complexation reactions was studied in NaCl and NaClO₄ media at two fixed ligand concentrations ($[\text{Lac}^-]_{\text{tot}} = 5.7 \times 10^{-1}; 3.5 \times 10^{-2} \text{ mol kg}^{-1}$) between 20 and 85 °C. The concentration of NaClO₄ was increased by successive titration using an aqueous 14.5 mol kg⁻¹ NaClO₄ solution. The $[\text{NaCl}]_{\text{tot}}$ was increased by addition of solid NaCl to the samples.

EXAFS spectroscopy: For EXAFS measurements samples with a total NpO_2^+ concentration of $5.0 \times 10^{-3} \text{ mol kg}^{-1}$ and a concentration of $[\text{Lac}^-]_{\text{tot}} = 2.5 \times 10^{-1} \text{ mol kg}^{-1}$ in H₂O were prepared. The ionic strength of all samples was adjusted to $I_m(\text{Na}^+, \text{Lac}^-/\text{Cl}^-) = 4.4 \text{ mol kg}^{-1}$ by addition of solid NaCl. The EXAFS experiments were conducted at various proton concentrations. The conditional pH_c values ($\text{pH}_c = 2.6 - 5.0$) were adjusted by addition of small aliquots of 6 mol L⁻¹ HCl (Merck, suprapure) or freshly prepared 1 mol L⁻¹ NaOH (Merck, Titrisol). The pH_c was measured by a combination pH electrode (Orion™ PerpHecT™ ROSS™), which was calibrated with pH reference buffer solutions (Merck, pH = 7.00, 5.00, 2.00). The volume of each sample was 200 μL.

ATR-FT-IR spectroscopy: The characteristic vibrational modes of the NpO_2^+ ion in solution are generally observed in the spectral range below 850 cm⁻¹ where strong interferences with modes of the bulk water (H₂O) occur.²² Therefore, deuterated water (D₂O, Sigma Aldrich, 99.9 atom % D, stored under argon) was used for the samples of the infrared spectroscopic experiments. All samples were prepared under inert gas atmosphere (N₂) to reduce the content of H₂O. The total NpO_2^+ concentration was $1.0 \times 10^{-3} \text{ mol kg}^{-1}$ and the ionic strength was $I_m = 1.0 \text{ mol kg}^{-1} (\text{Na}^+, \text{Lac}^-/\text{Cl}^-)$. NaCl was used as background electrolyte as it does not absorb light in the infrared region of interest. The total lactate concentration was $[\text{Lac}^-]_{\text{tot}} = 1.0 \times 10^{-1} \text{ mol kg}^{-1}$. The pD_c between 2.6 and 4.8 was adjusted by addition of small aliquots of 0.2 or 2 mol l⁻¹ DCl and 0.2 mol l⁻¹ NaOD in D₂O. For preparation of the respective acids and bases 35 wt. % DCl (Sigma Aldrich, 35 wt. % in D₂O, ≥ 99 atom % D) and 40 wt. % NaOD (Alfa Aesar, 40 wt.% in D₂O, 99.5 atom % D) were used. The pH values of the samples were determined and adjusted using an inoLab pH 720 pH-Meter (WTW, Weilheim, Germany) with a Blue Line 16pH microelectrode (Schott Instruments, Mainz, Germany). The calibration was performed using standard pH buffers (WTW, Weilheim, Germany) in H₂O. The pD_c values were corrected according to $\text{pD} = \text{pH} + 0.4$.²³ The NpO_2^+ concentration in the samples and the species distribution of the samples was confirmed by Vis/NIR spectroscopy. A Varian Cary 5G UV/Vis/NIR spectrophotometer was connected to the inert gas glove box via optical fibres to enable the characterization of the NpO_2^+ samples inside the glove box.

2.2 Vis/NIR absorption spectroscopy

The complexation of NpO_2^+ with lactate in aqueous solution was studied by NIR/Vis absorption spectroscopy between 20 and 85 °C using a Varian Cary 5G UV/Vis/NIR spectrophotometer. A Lauda Eco E100 thermostatic system was used to control the temperature of the sample holder. The samples

were equilibrated for 15 min at each temperature before measurement to ensure thermodynamic equilibrium. The spectra of the samples placed in quartz glass cuvettes (1 cm path length, Hellma Analytics) were recorded between 950 – 1050 nm with a data interval of 0.1 nm, a scan rate of 60 nm min⁻¹ (average accumulation time 0.1 s) and a slit width of 0.7 nm in double beam mode. For reference measurement and baseline correction samples at the same condition but without NpO₂⁺ were measured.

All uncertainties of the stability constants $\log \beta_n^0(T)$, enthalpies $\Delta_r H_{n,m}^0$, entropies $\Delta_r S_{n,m}^0$ and SIT binary ion-ion interaction coefficients $\Delta \epsilon_{j,k}$ determined in the present work are given with a confidence level of $1-\alpha = 0.95$.

2.3 EXAFS measurements

Np L₃-edge-EXAFS spectra were measured in fluorescence mode at an angle of 90° to the incident x-ray beam, using a 4 element Si SDD Vortex (SIINT) detector and an additional 1 element Si Vortex-60EX SDD (SIINT) fluorescence detector. The measurements were performed at the INE-Beamline of the *The Karlsruhe Research Accelerator* (KARA, Karlsruhe, Germany) which was equipped with a double-crystal monochromator (DCM; Ge(422) crystal pair) and a collimating and focusing mirror system (Rh-coated silicon mirrors). The flux of the incident beam was detuned in the middle of the scan range to 70 % peak intensity. An Ar-filled ionization chamber at ambient pressure was used to measure the intensity I_0 of the incident X-ray beam. All measurements in the EXAFS range were performed at equidistant k -steps and an increasing integration time following a \sqrt{k} progression. The measurements were performed at $T = 25$ °C. The software packages EXAFSPAK, Athena 0.8.056, and Artemis 0.8.012 were used for data evaluation.²⁴⁻²⁶ Theoretical scattering phases and amplitudes were calculated with FEFF8.40, using the crystal structures of UO₂ acetate and oxalate after replacement of the U-atom by Np.²⁷⁻²⁹ In all cases the k^2 - and k^3 -weighted raw EXAFS spectra were fitted.

2.4 ATR FT-IR spectroscopy

In situ ATR FT-IR spectroscopic measurements of the formed NpO₂⁺ lactate complexes were performed in D₂O. The spectra were measured on a Bruker Vertex 80/v vacuum spectrometer equipped with a mercury cadmium telluride (MCT) detector. The spectra were recorded between 4000 and 600 cm⁻¹ and averaged over 256 scans. The spectral resolution was 4 cm⁻¹. The used ATR unit DURA SamplIR II (Smiths Inc.), a horizontal diamond crystal with nine internal reflections on the upper surface and an angle of incidence of 45°, was purged with a current of dry air (dew point < 213 K). An ATR flow cell with a volume of 200 μ L was used to ensure adequate background subtraction without external thermal interference. The measurements were based on the principle of reaction-induced infrared difference spectroscopy. Here, infrared spectra of the solvent, the ligand solution and the samples containing NpO₂⁺ at equal experimental conditions (pH_c , I_m , temperature) were recorded in single

beam mode. Difference spectra were calculated from spectral data of the NpO_2^+ samples subtracting those of the reference samples exhibiting absorption changes caused by the complexation of the NpO_2^+ ion. Parts of the spectra which are unaffected by the complexation of NpO_2^+ , the strong absorbing background from the bulk water as well as contributions from the ATR FT-IR accessory and the instrument were eliminated displaying spectral features even due to minimal absorption changes ($\sim 10^{-5}$ OD).

2.5 Quantum chemical calculations

The TURBOMOLE 7.0 program package was used for quantum chemical calculations and structure optimizations of the NpO_2^+ lactate complexes.³⁰ The $\text{NpO}_2(\text{Lac})$ and $\text{NpO}_2(\text{Lac})_2^-$ complexes with different coordination modes (side-on vs. end-on) were optimized on the level of density functional theory (DFT) using the BH-LYP functional due to its better convergence compared to other hybrid-functionals.^{30, 31} All N, C, and H atoms were described by triple zeta basis sets (def-TZVP) and were treated at the all-electron level. The Np(V) ion was represented by a 60-electron core pseudo-potential (Np, ECP60MWB) with corresponding basis sets.³² The triplet spin state with two unpaired f-electrons resulting in a spin multiplicity of $S(S+1) = 2$ was used for all systems. The gas phase energies E_g were computed on MP2 level. Additionally, thermodynamic corrections ($E_{\text{vib}} = E_{\text{zp}} + H_0 - TS$, E_{zp} being the zero-point energy, H_0 and S are the enthalpies and entropies obtained from the calculations of the vibrational modes) and solvation energies E_{solv} (obtained using COSMO, $r(\text{Np}) = 1.72 \text{ \AA}$) were taken into account to obtain a theoretical approximation of the Gibbs free energies $G = E_g + E_{\text{vib}} + E_{\text{solv}}$.³³⁻³⁵ As the ligands and the NpO_2^+ ion are charged a full second hydration shell was added to avoid the charge of the complexes to contact the COSMO cavity. An application of ab-initio methods to optimize the structures of the NpO_2^+ complexes was not possible as the size of the systems was too big ($N > 100$ atoms) and the computation time was limited.

3 Results and Discussion

3.1 Vis/NIR absorption spectroscopy

3.1.1 Absorption Spectra

Figure 1 shows the absorption spectra of NpO_2^+ as a function of the total lactate concentration $[\text{Lac}^-]_{\text{tot}}$ at $T = 20$ and $85 \text{ }^\circ\text{C}$ and $I_m = 3.6 \text{ mol kg}^{-1} \text{ NaClO}_4$. At $20 \text{ }^\circ\text{C}$ the absorption band of the NpO_2^+ ion is located at $\lambda_{\text{max}} = 979.4 \text{ nm}$ ($\epsilon = 397 \pm 12 \text{ L mol}^{-1} \text{ cm}^{-1}$). With increasing $[\text{Lac}^-]_{\text{tot}}$ a bathochromic shift of the absorption spectra is observed. The Full Width at Half Maximum (FWHM) increases from 7.9 to 10.7 nm indicating the formation of NpO_2^+ lactate complex species.

With increasing temperature the absorption band of the NpO_2^+ ion shifts hypsochromically by 1.2 nm to 978.2 nm while the FWHM is unaffected by the temperature. The extinction coefficient decreases

to $\varepsilon = 362 \pm 15 \text{ L mol}^{-1} \text{ cm}^{-1}$. This blue shift is in good agreement to literature data. There, hypsochromic shifts by 1.5 – 1.9 nm are reported.³⁶⁻⁴⁰ At 85 °C the bathochromic shift observed at increasing ligand concentration is less pronounced compared to 20 °C. This is also reflected by a smaller increase of the FWHM from 7.9 to 10.4 nm. This indicates a reduced complex formation according to an exothermic complexation reaction.

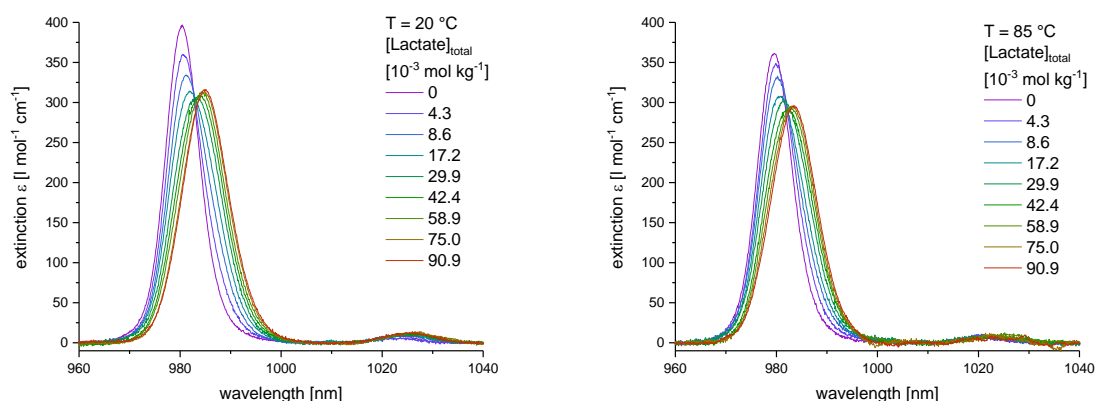


Figure 1: Absorption spectra of NpO_2^+ with increasing lactate concentration $[\text{Lac}]_{\text{tot}}$ at $T = 20 \text{ }^\circ\text{C}$ (left), and $T = 85 \text{ }^\circ\text{C}$ (right) and $I_m (\text{NaClO}_4) = 3.6 \text{ mol kg}^{-1}$.

The spectral changes and hypsochromic shifts of the NpO_2^+ ion with increasing temperature are contrary to the bathochromic shift induced by the complexation of NpO_2^+ at increasing $[\text{Lac}]_{\text{tot}}$. The effect of the temperature on the position of the absorption band of the NpO_2^+ ion has been discussed in the literature in detail.^{36, 37, 39, 41} Nevertheless, due to this effect, each series of spectra is evaluated separately and single component spectra must be determined for all experimental conditions.

3.1.2 Peak deconvolution and Speciation

The spectra of the formed NpO_2^+ lactate complexes are derived via subtractive deconvolution of the absorption spectra using the spectrum of the NpO_2^+ aquo ion. The spectra derived in NaClO_4 and NaCl media are identical at equal ionic strengths and temperatures. In Figure 2 the results of the peak deconvolution are presented for 20 and 85 °C in NaClO_4 ($I_m = 3.6 \text{ mol kg}^{-1}$). The absorption band of $\text{NpO}_2(\text{Lac})$ is located at $\lambda_{\text{max}} = 983.6 \text{ nm}$ ($\varepsilon = 356 \pm 12 \text{ L mol}^{-1} \text{ cm}^{-1}$), indicating a bathochromic shift of 4.2 nm compared to the absorption band of the NpO_2^+ aquo ion. The absorption band of $\text{NpO}_2(\text{Lac})_2^-$ is located at $\lambda_{\text{max}} = 987.1 \text{ nm}$ ($\varepsilon = 362 \pm 18 \text{ L mol}^{-1} \text{ cm}^{-1}$) and is shifted by 7.7 nm compared to the aquo ion. This shows, that each coordinating lactate ligand induces an average bathochromic shift of approximately 4.0 nm. At 85 °C all single component spectra are hypsochromically shifted by 1.2 nm whereas the integrated absorption coefficients remain constant. Thus, the absorption spectra of all Np(V) species are affected in the same way by changes of the temperature. Furthermore, at 85 °C the

single component spectrum of the $\text{NpO}_2(\text{Lac})_2^-$ complex could not be determined due to the low absorption intensity of this species and the unfavourable signal to noise ratio.

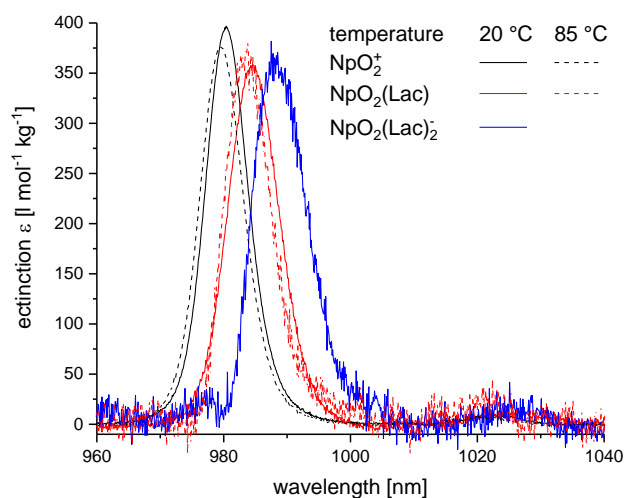


Figure 2: Absorption spectra of the NpO_2^+ ion and the $\text{NpO}_2(\text{Lac})_{n^{1-n}}$ ($n = 1, 2$) complexes at $T = 20$ (lines) and 85°C (dashed lines) and $I_m = 3.6 \text{ mol kg}^{-1} \text{ NaClO}_4$.

The deconvolution of the experimental absorption spectra is performed by principle component analyses using the pure component spectra.^{42, 43}

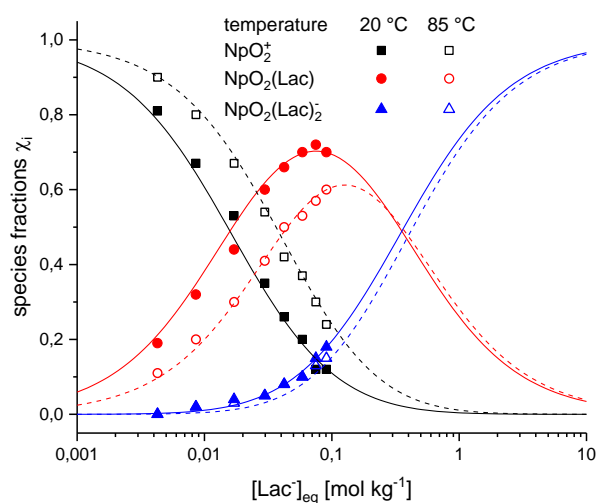


Figure 3: Experimentally determined (symbols) and calculated species distribution (lines) of $\text{NpO}_2(\text{Lac})_{n^{1-n}}$ ($n = 0, 1, 2$) complexes as a function of $[\text{Lac}^-]_{\text{eq}}$ in aqueous solution. $I_m = 3.6 \text{ mol kg}^{-1} \text{ NaClO}_4$; $T = 20^\circ\text{C}$ (solid lines) and 85°C (dashed lines).

The determined speciation of the NpO_2^+ lactate complexation is shown in Figure 3 (symbols) as a function of the equilibrium lactate concentration $[\text{Lac}^-]_{\text{eq}}$ at $T = 20$ and 85°C ($I_m = 3.6 \text{ mol kg}^{-1} \text{ NaClO}_4$). The calculated speciation according to the derived $\log \beta'_n(T)$ values are indicated as solid lines for 20°C and dashed lines for 85°C . $[\text{Lac}^-]_{\text{eq}}$ is calculated at each temperature according to the literature

procedure using the Henderson-Hasselbalch equation, SIT and the temperature dependence of the $pK_a^0(H^+ + L^- \rightleftharpoons HL)$ value.^{44, 45} The required standard reaction enthalpies and protonation constants are given in the literature.^{38, 44, 46-49} As no SIT parameters for the protonation reaction of Lac^- are available it is assumed that $\varepsilon(Na^+, Lac^-) = \varepsilon(Na^+, Ac^-) = 0.08 \pm 0.01$.⁵⁰

With increasing ligand concentration, the chemical equilibrium shifts towards the complexed species. For $[Lac^-]_{eq} > 1.6 \times 10^{-2} \text{ mol kg}^{-1}$ the $NpO_2(Lac)$ complex dominates the speciation. The $NpO_2(Lac)_2^-$ complex makes only a minor contribution to the species distribution at the experimental conditions. With increasing temperature the molar fractions of both lactate complexes decrease and the chemical equilibrium shifts towards the NpO_2^+ aquo ion. These trend shows that the complex formation is repressed at elevated temperatures indicating an exothermic complexation reaction of NpO_2^+ with lactate.

3.1.3 Complex stoichiometry

The stoichiometry of the formed complexes is determined by slope analyses at each studied temperature.^{51, 52} The slope analyses are performed according to the logarithmic form of the law of mass action (eqn. (1)).

$$\log \beta'_n = \log \frac{[NpO_2(Lac)_n]^{1-n}}{[NpO_2(Lac)_{n-1}]^{2-n}} - 1 \cdot \log[Lac^-]_{eq} \quad (1)$$

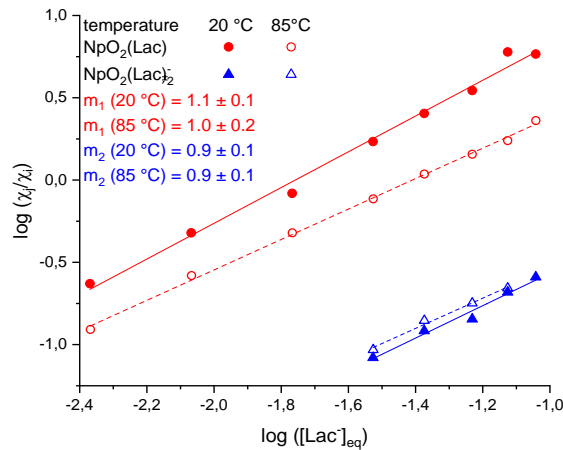


Figure 4: Plots of $\log \left(\frac{[NpO_2(Lac)_n]^{1-n}}{[NpO_2(Lac)_{n-1}]^{2-n}} \right)$ vs. $\log ([Lac^-]_{eq})$ and linear regression analyses according to eqn. (1) at 20 and 85 °C ($I_m = 3.6 \text{ mol kg}^{-1} \text{ NaClO}_4$).

The results of the slope analyses at $I_m = 3.6 \text{ mol kg}^{-1} \text{ NaClO}_4$ and $T = 20$ and 85 °C are displayed in Figure 4. The logarithmic molar fractions $\log \frac{[NpO_2(Lac)_n]^{1-n}}{[NpO_2(Lac)_{n-1}]^{2-n}}$ correlate linearly with $\log[Lac^-]_{eq}$ and linear regression analyses reveal slopes between 0.9 ± 0.1 and 1.1 ± 0.1 for all experimental conditions. Thus, the formation of two NpO_2^+ lactate complexes with a stoichiometry of $NpO_2(Lac)_n^{1-n}$ ($n = 1, 2$) is

confirmed. This result contrasts with solvent extraction studies by Moore et al reporting the formation of solely $\text{NpO}_2(\text{Lac})$ up to $[\text{Lac}^-]_{\text{tot}} = 0.1 \text{ mol kg}^{-1}$, $I_m = 0.3 - 5.0 \text{ mol kg}^{-1} \text{ NaCl}$ and $T = 25 \text{ }^\circ\text{C}$.¹⁸ This was confirmed by recent solvent extraction studies by Vasiliev et al.²⁰ In contrast to these studies, Inoue et al. reported the formation of $\text{NpO}_2(\text{Lac})_{n^{1-n}}$ ($n = 1, 2$) using absorption spectroscopy and solvent extraction at $1 \text{ mol L}^{-1} \text{ NaClO}_4$, $T = 25 \text{ }^\circ\text{C}$ and $[\text{Lac}^-]_{\text{tot}} = 2.0 \text{ mol L}^{-1}$ in the pH_c range of 5.8 to 7.5. These results are in good agreement with those of the present work.

3.1.4 Thermodynamic data

Using the experimental speciation data conditional $\log \beta'_n(T)$ values for the formation of $\text{NpO}_2(\text{Lac})_{n^{1-n}}$ ($n = 1, 2$) are determined at different temperatures and are extrapolated to $I_m = 0$ with the specific ion interaction theory (SIT) according to equation (3). Details on the SIT are given elsewhere.^{11, 12}

$$\log \beta' - \Delta z^2 D = \log \beta^0 + \Delta \epsilon I_m \quad (3)$$

The extrapolated $\log \beta^0_n(T)$ values are summarized in Table 1. At a given temperature the $\log \beta^0_n(T)$ values calculated for NaCl and NaClO₄ media are in good agreement within the error range. Hence, averaged values “ \emptyset ” for $\log \beta^0_n(T)$ are determined, yielding $\log \beta^0_1(20 \text{ }^\circ\text{C}) = 1.92 \pm 0.09$ for $\text{NpO}_2(\text{Lac})$ and $\log \beta^0_2(20 \text{ }^\circ\text{C}) = 2.10 \pm 0.06$ for $\text{NpO}_2(\text{Lac})_2^-$. With increasing temperature, the first stability constant decreases by 0.12 logarithmic units to $\log \beta^0_1(85 \text{ }^\circ\text{C}) = 1.80 \pm 0.14$. The second stability constant decreases by 0.17 logarithmic units to $\log \beta^0_2(85 \text{ }^\circ\text{C}) = 1.93 \pm 0.15$. The decrease in the stability constants shows that the complexation of NpO_2^+ with lactate is exothermic. The standard reaction enthalpy $\Delta_r H^0_{n,m}$ and entropy $\Delta_r S^0_{n,m}$ are determined by plotting the averaged $\log \beta^0_n(T)$ versus the reciprocal temperature T^{-1} . The data correlate linearly with T^{-1} and the temperature dependence is described by the integrated Van't Hoff equation (eqn. (4)) (see Figure 5).

$$\log \beta^0_n(T) = \log \beta^0_n(T_0) + \frac{\Delta_r H^0_m(T_0)}{R \ln(10)} \left(\frac{1}{T_0} - \frac{1}{T} \right) \quad (4)$$

R is the universal gas constant and T the absolute temperature. $T_0 = 298.15 \text{ K}$ is the temperature of the IUPAC reference state. The Van't Hoff equation is only valid for a small temperature range of about $\Delta T = 100 \text{ K}$ assuming $\Delta_r C^0_{m,p} = 0$ and $\Delta_r H^0_m = \text{const}$.

Table 1: Thermodynamic stability constants $\log \beta^0_n(T)$ for the formation of $\text{NpO}_2(\text{Lac})_{n^{1-n}}$ ($n = 1, 2$) obtained in NaClO₄ and NaCl media and their mean values “ \emptyset ” as a function of temperature. Confidence interval: $1-\alpha = 0.95$. \emptyset : mean values

	T [°C]	20	30	40	50	60	70	80	85
[NpO ₂ (Lac)]	NaClO ₄	1.87 ±	1.88 ±	1.85 ±	1.81 ±	1.76 ±	1.75 ±	1.73 ±	1.73 ±
	\emptyset	0.08	0.07	0.09	0.09	0.10	0.05	0.13	0.10

[NpO ₂ (Lac) ₂] ⁻	NaCl	1.96 ± 0.06	1.95 ± 0.09	1.92 ± 0.09	1.90 ± 0.08	1.86 ± 0.08	1.85 ± 0.11	1.81 ± 0.09	1.86 ± 0.13
		∅	1.92 ± 0.09	1.92 ± 0.11	1.88 ± 0.12	1.85 ± 0.11	1.81 ± 0.13	1.80 ± 0.12	1.77 ± 0.15
	NaClO ₄	2.04 ± 0.08	2.02 ± 0.09	2.00 ± 0.08	1.96 ± 0.09	1.90 ± 0.12	1.89 ± 0.12	1.86 ± 0.15	1.85 ± 0.15
		∅	2.10 ± 0.06	2.09 ± 0.11	2.05 ± 0.12	2.01 ± 0.06	1.96 ± 0.09	1.95 ± 0.16	1.91 ± 0.09
	NaCl	2.16 ± 0.06	2.15 ± 0.12	2.10 ± 0.15	2.07 ± 0.09	2.03 ± 0.11	2.03 ± 0.15	1.97 ± 0.09	2.02 ± 0.14
		∅	2.10 ± 0.06	2.09 ± 0.11	2.05 ± 0.12	2.01 ± 0.06	1.96 ± 0.09	1.95 ± 0.16	1.91 ± 0.09

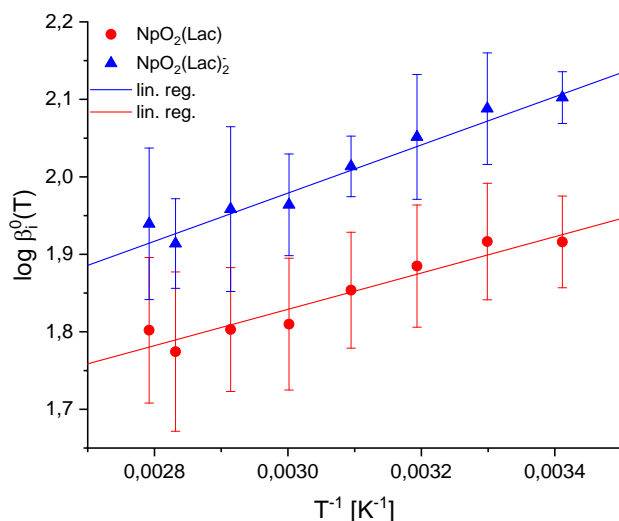


Figure 5: $\log \beta_n^0(T)$ ($n = 1, 2$) as a function of the reciprocal temperature and fitting according to the integrated Van't Hoff equation (eqn. 4). Confidence interval: $1-\alpha = 0.95$.

The obtained $\Delta_r H_{n,m}^0$ and $\Delta_r S_{n,m}^0$ values are listed in Table 2. The formation of both complexes is slightly exothermic in both electrolytes (NaCl and NaClO₄). The averaged standard reaction enthalpies are $\Delta_r H_{1,m}^0(\text{NpO}_2(\text{Lac})) = -4.5 \pm 0.5 \text{ kJ mol}^{-1}$ and $\Delta_r H_{2,m}^0(\text{NpO}_2(\text{Lac})_2^-) = -6.0 \pm 0.4 \text{ kJ mol}^{-1}$, the standard reaction entropies are $\Delta_r S_{1,m}^0(\text{NpO}_2(\text{Lac})) = 22 \pm 5 \text{ J mol}^{-1} \text{ K}^{-1}$ and $\Delta_r S_{2,m}^0(\text{NpO}_2(\text{Lac})_2^-) = 20 \pm 6 \text{ J mol}^{-1} \text{ K}^{-1}$.

Table 2: Thermodynamic functions of the formation of $\text{NpO}_2(\text{Lac})_n^{1-n}$ ($n = 1, 2$). Confidence interval: $1-\alpha = 0.95$. ∅: mean values

electrolyte	$\text{NpO}_2(\text{Lac})_n^{1-n}$	$\log \beta_n^0(25 \text{ °C})$	$\Delta_r H_{n,m}^0 [\text{kJ mol}^{-1}]$	$\Delta_r S_{n,m}^0 [\text{J mol}^{-1} \text{K}^{-1}]$	$\Delta \epsilon$
-------------	------------------------------------	---------------------------------	---	--	-------------------

NaClO₄	n = 1	1.87 ± 0.11	-4.2 ± 0.3	19 ± 4	-0.09 ± 0.07
	n = 2	2.03 ± 0.12	-5.8 ± 0.5	22 ± 5	-0.11 ± 0.06
NaCl	n = 1	1.96 ± 0.11	-4.8 ± 0.4	21 ± 4	-0.12 ± 0.05
	n = 2	2.15 ± 0.13	-6.2 ± 0.3	22 ± 3	-0.11 ± 0.03
∅	n = 1	1.92 ± 0.14	-4.5 ± 0.5	22 ± 5	
	n = 2	2.10 ± 0.13	-6.0 ± 0.4	20 ± 6	

In the literature only two $\log \beta_1^0(25\text{ }^\circ\text{C})$ values are reported determined by solvent extraction techniques.¹⁸ Moore et al. determined $\log \beta_1^0(25\text{ }^\circ\text{C}) = 1.70$ for the formation of $\text{NpO}_2(\text{Lac})$ by application of the SIT and $\log \beta_1^0(25\text{ }^\circ\text{C}) = 1.97$ by application of the Pitzer model. Both values are in very good agreement with the $\log \beta_1^0(25\text{ }^\circ\text{C})$ value in the present work. The formation of higher complex species is not described in this survey. A recent study by Vasiliev et al. provides a stability constant for $\text{NpO}_2(\text{Lac})$ of $\log \beta_1^0(25\text{ }^\circ\text{C}) = 1.96 \pm 0.05$ as well as $\Delta_r H_{1,m}^0(\text{NpO}_2(\text{Lac})) = -5.4 \pm 1.4\text{ kJ mol}^{-1}$ and $\Delta_r S_{1,m}^0(\text{NpO}_2(\text{Lac})) = 19 \pm 4\text{ kJ mol}^{-1}$.²⁰ These results are in excellent agreement with those of the present work. Nevertheless, due to the lower total lactate concentration the formation of higher complex species was not observed by Vasiliev et al. In addition, conditional stability constants for $\text{NpO}_2(\text{Lac})_n^{-1n}$ ($n = 1, 2$) are determined by Inoue et al. at $I = 1\text{ mol L}^{-1}\text{ NaClO}_4$ and $T = 25\text{ }^\circ\text{C}$.^{19, 53} In table 3, these constants are compared to the results of the present work at identical chemical conditions. The spectrophotometrically determined $\log \beta'_1$ is in good agreement with the one of the present work whereas the values determined by both solvent extraction studies are significantly lower. Furthermore, different complex species were identified by Inoue et al. within the different experimental approaches.^{19, 53} The solvent extraction experiments reveal the formation of $\text{NpO}_2(\text{Lac})_n^{-1n}$ ($n = 1, 2$), while the spectroscopic study suggests the exclusive formation of $\text{NpO}_2(\text{Lac})$. This might explain the huge deviations of the $\log \beta'_1$ values obtained by Inoue et al. with the two different experimental methods.

Table 3: Conditional stability constants for the complexation of NpO_2^+ with lactate at $I_m = 1.0\text{ mol kg}^{-1}$ (NaClO_4) and $T = 25\text{ }^\circ\text{C}$.

method	$\log \beta'_{01}$	$\log \beta'_{02}$	reference
--------	--------------------	--------------------	-----------

A	1.11 ± 0.08	1.78 ± 0.03	19
R	1.09	1.60	53
sp	1.75	-	19
sp	1.88 ± 0.08	2.02 ± 0.09	p.w.

A: solvent extraction with thenoyl-trifluoroacetone (TTA) and 1,10-phenantroline (Phen); organic diluent: iso-butylmethylketone. **R:** solvent extraction with TTA and alkylammonium; organic diluent: benzene. **sp:** spectrophotometry. **p.w.:** present work.

Furthermore, comparison of the present results with results on the complexation of NpO_2^+ with the structurally related carboxylate “propionate” reveals the effect of the α -OH group on the thermodynamic functions. Solvent extraction studies by Vasiliev et al. report $\log \beta_1^0(\text{NpO}_2(\text{Prop}), 25^\circ\text{C}) = 1.19 - 1.26$, $\Delta_r H_{1,m}^0(\text{NpO}_2(\text{Prop})) = 10.9 - 16.3 \text{ kJ mol}^{-1}$ and $\Delta_r S_{1,m}^0(\text{NpO}_2(\text{Prop})) = 62 - 77 \text{ J mol}^{-1} \text{ K}^{-1}$.^{20, 54} Comparison with the present results for $\text{NpO}_2(\text{Lac})$ shows that the additional α -OH group results in an increase of the complex stability accompanied with a lowering of $\Delta_r H_{1,m}^0$. This points to significant differences in the coordination mode of both ligands. Propionate coordinates end-on towards NpO_2^+ whereas lactate can form chelate complexes involving the COO^- and OH group.

The application of the SIT yields the stoichiometric sum of the binary ion-ion interaction coefficients $\Delta \varepsilon_{j,k}$ of the complex formations. In Figure 6 the determined $\Delta \varepsilon_{01}$ and $\Delta \varepsilon_{02}$ values are displayed as a function of the temperature for the reaction $\text{NpO}_2^+ + n \text{ Lac}^- \rightleftharpoons \text{NpO}_2(\text{Lac})_n^{1-n}$ ($n = 1, 2$) in NaClO_4 and NaCl media. No temperature dependence of the $\Delta \varepsilon_{j,k}$ values is observed in NaClO_4 . In NaCl $\Delta \varepsilon_{01}$ increases slightly whereas $\Delta \varepsilon_{02}$ remains constant. However, the temperature dependence is negligible within the error range of the data. Various studies on the ionic strength dependence of complexation reactions of trivalent lanthanides and actinides showed, that the effect of temperature on $\Delta \varepsilon_{j,k}$ is rather small and thus negligible in the temperature range of 20 to 90 °C.^{46, 51, 54} Recent studies on the complexation of Np(V) with sulphate, fluoride, formate and acetate support these observations.^{38-40, 55} Thus, temperature independent $\Delta \varepsilon_{j,k}$ values are calculated for NaClO_4 and NaCl media (Table 2). The averaged values are $\Delta \varepsilon_{01}(\text{NaClO}_4) = -0.09 \pm 0.02$, $\Delta \varepsilon_{01}(\text{NaCl}) = -0.12 \pm 0.02$ and $\Delta \varepsilon_{02}(\text{NaClO}_4) = -0.20 \pm 0.03$, $\Delta \varepsilon_{02}(\text{NaCl}) = -0.23 \pm 0.02$. In order to derive the binary ion-ion interaction coefficients $\varepsilon_{j,k}$ of the different NpO_2^+ lactate complexes with both background electrolytes the following parameters stated in the NEA-TDB are used: $\varepsilon(\text{Na}^+, \text{Lac}^-) \approx \varepsilon(\text{Na}^+, \text{Ac}^-) = 0.08 \pm 0.01$, $\varepsilon(\text{NpO}_2^+, \text{ClO}_4^-) = 0.25 \pm 0.05$ and $\varepsilon(\text{NpO}_2^+, \text{Cl}^-) = 0.09 \pm 0.05$.¹¹ The $\varepsilon(\text{Na}^+ + \text{Cl}^-/\text{ClO}_4^-, \text{NpO}_2(\text{Lac}))$ and $\varepsilon(\text{Na}^+, \text{NpO}_2(\text{Lac})_2^-)$ values are calculated according to equation (5).

$$\Delta\varepsilon = \sum \varepsilon_{products} - \sum \varepsilon_{educt} \quad (5)$$

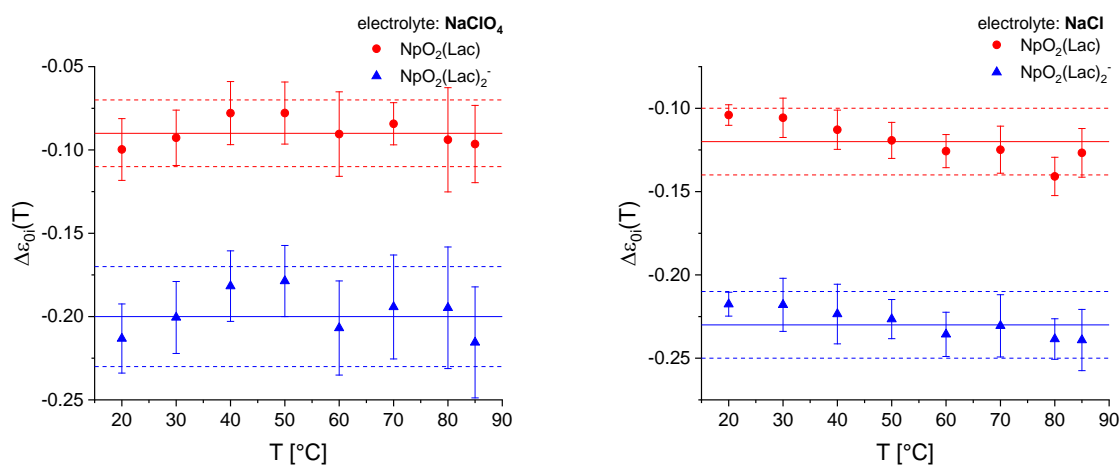
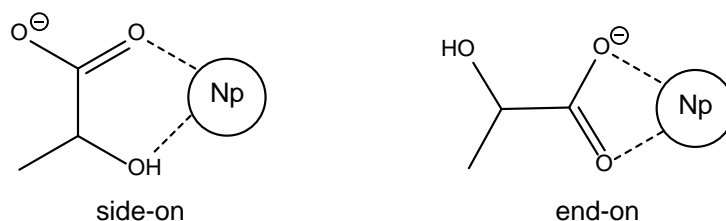


Figure 6: $\Delta\varepsilon_{i,k}(T)$ values for the reaction $\text{NpO}_2^+ + n \text{Lac} \rightleftharpoons \text{NpO}_2(\text{Lac})_{n-1-n}$ ($n = 1, 2$) in NaClO_4 (left) and NaCl (right) as a function of the temperature. The error of the mean value (solid line) is represented by the dashed lines.

The SIT binary ion-ion interaction parameters for $\text{NpO}_2(\text{Lac})$ are $\varepsilon(\text{Na}^+ + \text{ClO}_4^-, \text{NpO}_2(\text{Lac})) = 0.24 \pm 0.06$ and $\varepsilon(\text{Na}^+ + \text{Cl}^-, \text{NpO}_2(\text{Lac})) = 0.05 \pm 0.05$. For $\text{NpO}_2(\text{Lac})_2^-$ the parameters are $\varepsilon(\text{Na}^+, \text{NpO}_2(\text{Lac})_2^-) = 0.21 \pm 0.06$ determined in NaClO_4 and $\varepsilon(\text{Na}^+, \text{NpO}_2(\text{Lac})_2^-) = 0.02 \pm 0.05$ determined in NaCl . According to the SIT it is assumed that $\varepsilon_{j,k} = 0$ for uncharged species. Taking into account the error of the $\varepsilon_{j,k}$ values, this is the case for $\varepsilon(\text{Na}^+ + \text{Cl}^-, \text{NpO}_2(\text{Lac}))$. However, $\varepsilon(\text{Na}^+ + \text{ClO}_4^-, \text{NpO}_2(\text{Lac}))$ deviates significantly from zero. Similar deviations were observed for the complexes of NpO_2^+ with formate, acetate, fluoride and chloride in NaClO_4 media.^{38,40,41,55} It is assumed that the $\varepsilon(\text{NpO}_2^+, \text{ClO}_4^-) = 0.25 \pm 0.05$ given in the NEA-TDB is defective and should be re-evaluated.¹¹ Nonetheless, the thermodynamic functions ($\log \beta_n^0(T)$, $\Delta_r H_{n,m}^0$, $\Delta_r S_{n,m}^0$) obtained for both electrolytes (NaCl and NaClO_4) are in excellent agreement and thus the ionic strength dependence of the complex formations is accurately described in the present work.

3.2 Structural characterization of the $\text{NpO}_2(\text{Lac})_{n-1-n}$ complexes

For α -hydroxy carboxylates two coordination modes towards the NpO_2^+ ion are possible (see scheme 1). Information on the structure of the $\text{NpO}_2(\text{Lac})_{n-1-n}$ complexes should show if the α -OH group is involved in the complexation of An(V) ions and how this might affect the thermodynamic behaviour.



Scheme 1: Possible coordination modes of lactate towards the NpO_2^+ center. (left) side-on coordination with a monodentate binding of the COO^- group, (right) end-on coordination with a bidentate binding of the COO^- group

3.2.1 EXAFS spectroscopy

The k^2 -weighted Np-L₃-edge EXAFS spectra of NpO₂⁺ in the presence of lactate, the Fourier transformations and the corresponding fit curves are given in the ESI in figure S1 as a function of the pH_c value. The results of the fits and the fit parameters are listed in Table S1 in the ESI. A summary of the obtained structural parameters is given in Table 4. The spectra are dominated by the axial and equatorial O-atoms (O_{ax}, O_{eq}). The averaged distance of the axial O-atoms (O_{ax}) is 1.84 ± 0.01 Å and of the equatorial O-atoms (O_{eq}) 2.49 ± 0.02 Å. The coordination number of the NpO₂⁺ ion in the equatorial plane varies between 3.1 and 4.9. Both, the coordination numbers and the distances of the O-atoms are not affected by the pH_c value. Furthermore, the results are in excellent agreement with literature data.^{56, 57}

The coordination mode of the lactate molecules towards the NpO₂⁺ ion is determined by evaluating the distances of the carbon atoms of the coordinating functional groups (-COO⁻ and -COH). At pH_c = 0.8 no lactate complexes are formed and the spectrum corresponds to the solvated NpO₂⁺ ion. At pH_c = 2.6 the evaluation of the EXAFS spectrum reveals 1.3 carbon atoms C_c at 2.72 ± 0.08 Å from the Np(V) center. With increasing pH_c up to 5.2 both, the number of carbon atoms and the C_c distance increase from 1.3 – 2.5 and from 2.72 ± 0.08 - 3.23 ± 0.02 Å, respectively. This indicates a change of the coordination mode of lactate with increasing basicity.

Table 4: Structural parameters for the NpO₂(Lac)_n¹⁻ⁿ (n = 1, 2) complexes obtained from the fits of the raw k^2 -weighted Np-L₃-edge EXAFS spectra shown in Fig. S1. *fixed for fitting.

pH		0.8	2.6	3.3	4.0	4.7	5.2
O _{ax}	N	2*	2*	2*	2*	2*	2*
	R / Å	1.83 (1)	1.85 (1)	1.83 (1)	1.84 (1)	1.84 (1)	1.84 (1)
O _{eq}	N	4.9 (1)	3.1 (1)	4.2 (1)	4.1 (1)	4.2 (1)	4.1 (1)
	R / Å	2.48 (1)	2.51 (2)	2.49 (1)	2.49 (1)	2.48 (1)	2.48 (1)
C _{coord}	N	-	1.3 (1)	1.1 (1)	1.2 (1)	1.3 (1)	2.5 (1)
	R / Å	-	2.72 (8)	2.81 (4)	3.12 (4)	3.14 (2)	3.23 (2)

Takao et al. studied the complexation of NpO₂⁺ with acetate by EXAFS spectroscopy.⁵⁸ In this study a C_c distance of 2.91 ± 0.02 Å between the NpO₂⁺ center and the coordinating COO⁻ group is reported. In an EXAFS study on Np-propionate complexes by Vasiliev et al. a C_c distance of 2.87 ± 0.03 Å was determined.⁵⁴ These distances obtained for monocarboxylic ligands serve as reference for an end-on

coordination mode of the COO^- group via the two O-atoms. Furthermore, the C_c distances obtained for NpO_2^+ complexes are in good agreement with structural parameters of Am(III)-acetate complexes.⁵⁹ There, a C_c distance of $2.82 \pm 0.05 \text{ \AA}$ to the americium ion was determined. Literature data on structural parameters of Am(III) lactate complexes show, that the distal C_c atoms are located at $3.42 \pm 0.03 \text{ \AA}$.⁴⁴ This is distinctively larger compared to the distance in the Am(III) acetate complexes and indicates a side-on coordination of lactate with the formation of a five-membered chelate ring at $\text{pH}_c \geq 3.0$.

The comparison with the known C_c distances for side-on and end-on coordination indicates that at low pH_c lactate coordinates only via the COO^- -group towards NpO_2^+ . With increasing pH_c the C_c distance increases and the coordination mode changes to a side-on coordination of lactate via the COO^- - and COH -group. Thus, the proton concentration has a major effect on the coordination mode of lactate towards the NpO_2^+ ion.

3.2.2 ATR FT-IR spectroscopy

The vibrational modes of the coordinated ligand and the NpO_2^+ ion provides additional information on the structure of the complexes and the coordination mode of lactate towards the NpO_2^+ ion.

Prior to the measurement of the NpO_2^+ lactate samples, the vibrational spectra of the pure ligand at identical experimental conditions are recorded (Fig. 7, top). All spectra are dominated by bands at 1716, 1587 and 1416 cm^{-1} representing the vibrational modes of the COOH group as well as the symmetric ($\nu_s(\text{COO}^-)$) and anti-symmetric ($\nu_{as}(\text{COO}^-)$) modes of the COO^- group. The absorption bands at 1462 and 1116 cm^{-1} corresponds to the $\nu_{\text{AL}}(\text{OH})$ and $\nu_{\text{AL}}(\text{CO})$ modes of the COH group. These values are in good agreement with literature data.^{60, 61}

The infrared spectra of the NpO_2^+ lactate species at various pD_c values ($\text{pD}_c = 2.6, 4.1, 4.8$) are shown in Fig. 7 (bottom)(difference spectra after subtraction of the spectra of the pure ligand). The absorption spectra show a contribution of the free lactic acid which is represented by the negative absorption band at 1716 cm^{-1} . Modes of the ligand undergoing alterations upon complexation are detected as positive absorption bands at 1587, 1456, 1416 and 1100 cm^{-1} .

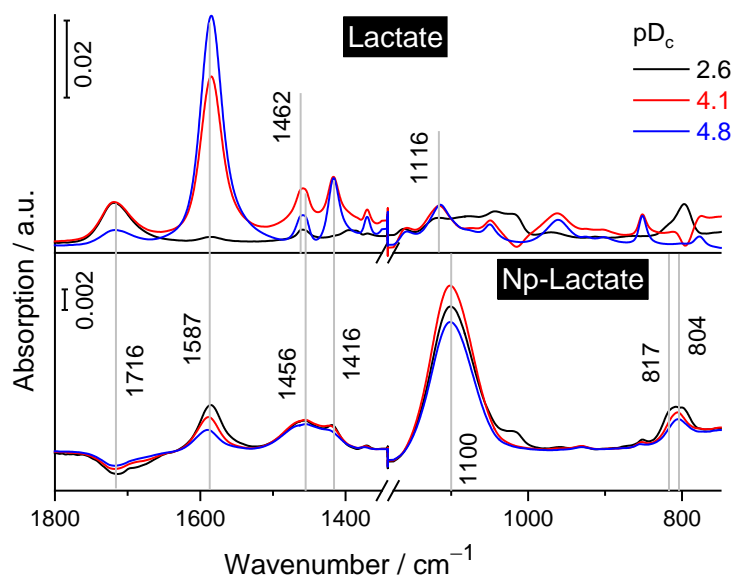


Figure 7: ATR-FT infrared spectra of the pure lactate (top) and the difference spectra of the NpO_2^+ lactate samples (bottom) as a function of the pD_c value. $I_m(\text{NaCl}) = 1.0$, $T = 20^\circ\text{C}$, $[\text{NpO}_2^+]_{\text{total}} = 2.0 \times 10^{-3} \text{ mol kg}^{-1}$, $[\text{Lac}^-]_{\text{total}} = 0.1 \text{ mol kg}^{-1}$.

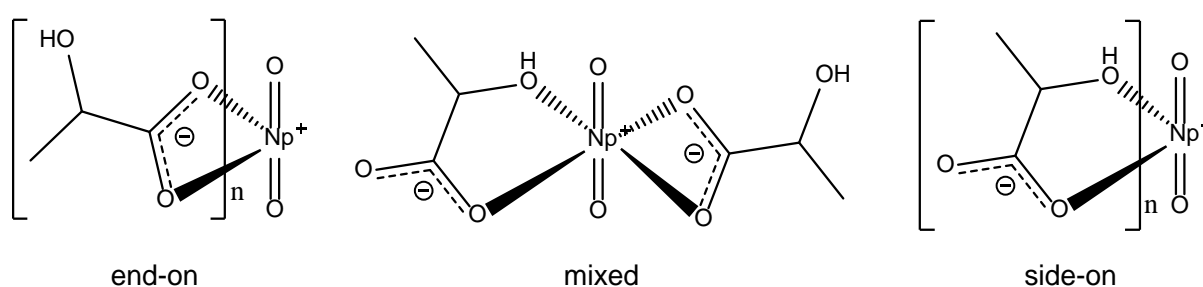
The vibrational band of the $\nu_3(\text{NpO}_2)$ mode is observed in the spectral region below 850 cm^{-1} .²² Its frequency and shape changes slightly as a function of the pD_c value. Thus, a deconvolution of this band was performed, and frequencies of single species were obtained from second derivative spectra (data not shown). At $\text{pD}_c = 2.6$, two bands at 799 and 817 cm^{-1} are observed. The first one represents the OD mode of the free lactate. The band at 817 cm^{-1} is assigned to the free NpO_2^+ ion.^{22, 62} Thus, at $\text{pD}_c = 2.6$ the NpO_2^+ aquo ion is the predominant species. An increasing number of coordinated lactate molecules in the equatorial plane of the NpO_2^+ ion lowers the frequency of the antisymmetric stretching vibration. Consequently, upon increasing the pD_c value to 4.1 a vibrational band at 804 cm^{-1} is obtained corresponding to a single species, NpO_2Lac . This band remains unchanged in the spectrum obtained at $\text{pD}_c = 4.8$. Thus, the frequency of the $\nu_3(\text{NpO}_2)$ mode provides information on the number of different complex species but no direct indication of the coordination mode of the ligand.

However, information on the coordination mode of the ligand to the NpO_2^+ ion can be derived from the antisymmetric and symmetric stretching modes of the carboxylic groups ($\nu_{\text{as}}(\text{COO}^-)$ and $\nu_{\text{s}}(\text{COO}^-)$). Their spectral splitting ($\Delta\nu$) allows a differentiation between bidentate and monodentate coordination of the COO^- group to the metal ion.^{63, 64} Generally, a bidentate coordination is characterized by a smaller splitting ($\Delta\nu < 100 \text{ cm}^{-1}$) whereas a monodentate binding results in a larger spectral splitting ($\Delta\nu > 150 \text{ cm}^{-1}$).⁶⁴ The vibrational modes of the COO^- group of the lactate ligand have nearly the same frequency values throughout the whole pD_c range investigated, that are 1587 cm^{-1} for the $\nu_{\text{as}}(\text{COO}^-)$ and 1416 cm^{-1} for the $\nu_{\text{s}}(\text{COO}^-)$ mode. Therefore, the constant value $\Delta\nu$ of about 171 cm^{-1} suggests a monodentate coordination of the COO^- group in the series of the NpO_2^+ lactate spectra excluding an end-on coordination of the ligand towards the NpO_2^+ ion (compare scheme 1). Furthermore, the

comparison of the spectral data shown in figure 7 (top) and (bottom) reveals that the impact of replacing the monovalent Na^+ by NpO_2^+ on the vibrational modes of the COO^- group is not significant. In contrast, a shift of the alcoholic $\nu_{\text{AL}}(\text{CO})$ band from 1116 to 1100 cm^{-1} and of $\nu_{\text{AL}}(\text{OH})$ from 1462 to 1456 cm^{-1} is observed indicating that the COH group is involved in the binding of lactate towards NpO_2^+ .⁶⁰ This shift is unaffected by the pD_c value. According to the EXAFS results with increasing pH_c/pD_c a change of the coordination mode from side-on to end on is expected. This is not observed by the infrared spectroscopy. However, the infrared spectra are in good agreement with the results obtained by EXAFS at higher pH_c values indicating a side-on coordination of lactate towards the NpO_2^+ ion.

3.2.3 Quantum chemical calculations

The molecular structures of different constitution isomers of the $\text{NpO}_2(\text{Lac})$ and $\text{NpO}_2(\text{Lac})_2^-$ complexes (see Scheme 2) are optimized on DFT level using the BH-LYP functional and def-TZVP basis sets.³⁰⁻³² The calculated bond distances are summarized in table 5 and compared to the results of the EXAFS evaluation. The data show that the bond distances of the axial and equatorial O-atoms (O_{ax} , O_{eq}) are not affected by the coordination mode of the ligand. Thus, it is not possible to differentiate between the coordination modes of the lactate molecule using the distances of O_{ax} or O_{eq} towards the NpO_2^+ center. However, the distances of the C-atoms C_c of the COO^- and COH-group differ significantly for end-on and side-on coordination. For the end-on coordinated lactate a C_c distance of 2.91 Å is calculated which is about 0.48 Å shorter compared to the C_c distance of the side-on coordinated ligand molecule ($\text{C}_c = 3.39$ Å).



Scheme 2: Schematic structures of the different constitution isomers of the NpO_2^+ lactate complexes. Water molecules are omitted for clarity.

Table 5: Distances of the O_{ax} , O_{eq} and C_c towards the metal centre. Experimental EXAFS results and quantum chemical calculations.

method	complex	Coord.mode	O_{ax} [Å]	O_{eq} [Å]	C_c [Å]
DFT	$\text{NpO}_2(\text{Lac})$	End-on	1.83	2.49	2.91
		Side-on	1.84	2.46	3.39

	$\text{NpO}_2(\text{Lac})_2^-$	End-on	1.81	2.47	2.92
		Side-on	1.84	2.45	3.39
		Mixed	1.84	2.47	2.86 / 3.40
EXAFS	$\text{NpO}_2(\text{Lac})/$ $\text{NpO}_2(\text{Lac})_2^-$		1.84	2.47	2.72 – 3.32

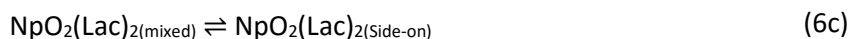
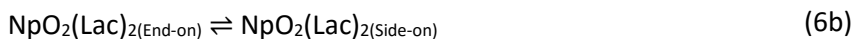
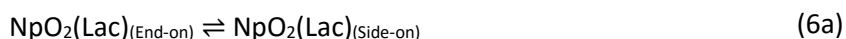
The comparison with the experimentally obtained distances shows that the calculated values for O_{ax} and O_{eq} are in excellent agreement with the experimental results. However, the C_c distance determined by EXAFS spectroscopy increase with increasing pH_c from 2.98 up to 3.38 Å. The distance at low pH_c is in good agreement with the calculated distance for the end-on coordinating lactate. The experimentally determined C_c distance at $pH_c = 4.9$ agrees with the distance for the side-on coordinating lactate via the COO^- and COH group. Unfortunately, the quantum chemical calculations do not account for pH_c effects. Nevertheless, the calculations confirm the experimentally observed C_c distances for the end-on and the side-on coordination mode of lactate.

Table 6: Gibbs free energies for the isomerisation of $\text{NpO}_2(\text{Lac})_n^{1-n}$ ($n = 1, 2$) according to eqn (6a-c). Ground state energies calculated on MP2 level.

complex	ΔE_g [kJ mol ⁻¹]	ΔE_{vib} [kJ mol ⁻¹]	ΔE_{comso} [kJ mol ⁻¹]	ΔG [kJ mol ⁻¹]	eqn.
$\text{NpO}_2(\text{Lac})$	-4.20	20.15	6.01	39.89	(6a)
$\text{NpO}_2(\text{Lac})_2^-$	28.13	-28.26	-18.58	-18.71	(6b)
	-28.90 ^a	1.11 ^a	23.85 ^a	-3.93 ^a	(6c)

a) $\Delta E = \Delta E_{\text{Side-on}} - \Delta E_{\text{mixed}}$

Calculations of the Gibbs free energies ΔG provide additional information on the coordination mode of lactate towards NpO_2^+ . The Gibbs energies for the isomerisation of $\text{NpO}_2(\text{Lac})_n^{1-n}$ ($n = 1, 2$) are calculated according to eqn. (6a-c).



ΔG is calculated using the difference of the ground state energies ΔE_g on MP2 level while thermodynamic corrections ΔE_{vib} and solvation effects ΔE_{COSMO} are considered: $\Delta G = \Delta E_g + \Delta E_{vib} + \Delta E_{COSMO}$. The results show, that in case of the isomerisation of $NpO_2(Lac)$ ΔG is positive, whereas it is negative for $NpO_2(Lac)_2^-$ (see table 6). Thus, for the 1:1 complex the end-on coordination of the ligand is more stable compared to the side-on coordination. In contrast, for the 1:2 complex the formation of chelate complexes is energetically preferred. Furthermore, the 1:2 complex with two lactate molecules forming chelate rings is more stable compared to the mixed structure (see Scheme 2). This is expressed by the more negative ΔG value for the isomerisation according to eqn. (6b) in comparison to eqn. (6c). The quantum chemical calculations do not consider effects of the proton concentration on the coordination mode of lactate. Nevertheless, the results confirm the general trend observed by EXAFS of changing coordination modes with increasing pH_c . An increasing pH_c results in a shift of the chemical equilibrium towards the $NpO_2(Lac)_2^-$ complex. At low pH_c $NpO_2(Lac)$ is the predominant species and the coordination mode of lactate is end-on. The $NpO_2(Lac)_2^-$ complex becomes more prominent at higher pH_c and the results by EXAFS reveal the side-on coordination. This is in good agreement with the theoretical approximations of ΔG . However, pH_c effects on the coordination mode cannot experimentally be studied without affecting the species distribution.

4 Summary

In the present work the thermodynamics and structures of the complexes of NpO_2^+ with lactate are investigated by different techniques such as absorption spectroscopy, EXAFS spectroscopy, ATR-FT infrared spectroscopy and quantum chemical calculations. The formation of the NpO_2^+ lactate complexes is studied photometrically as a function of the ligand concentration (Lac^-), ionic strength (NaCl and NaClO₄) and temperature (20 – 85 °C). Two different complex species are observed which are identified as $NpO_2(Lac)$ and $NpO_2(Lac)_2^-$. With increasing temperature, the equilibrium of the complex formation shifts towards the NpO_2^+ aquo ion. $\log \beta_1^0(20\text{ °C}) = 1.92 \pm 0.09$ decreases by 0.12 and $\log \beta_2^0(20\text{ °C}) = 2.10 \pm 0.06$ decreases by 0.17 in the temperature range of 20 – 85 °C. Correlation of $\log \beta_n^0(T)$ with the reciprocal temperature and fitting according to the integrated Van't Hoff equation yield the standard reaction enthalpies ($\Delta_r H_{n,m}^0$) and entropies ($\Delta_r S_{n,m}^0$) of the complexation reactions. Linear regression analyses reveal $\Delta_r H_{1,m}^0 = -4.5 \pm 0.5$ and $\Delta_r H_{2,m}^0 = -6.0 \pm 0.4$ confirming slightly exothermic complexation reactions.

The $\Delta \varepsilon_{01}$ and $\Delta \varepsilon_{02}$ values are determined as a function of temperature for two different ionic media (NaCl and NaClO₄). No significant temperature dependence of $\Delta \varepsilon_{01}$ and $\Delta \varepsilon_{02}$ is observed and averaged, temperature independent values are used to determine $\varepsilon_{j,k}$ values of the NpO_2^+ -lactate complexes with the two different electrolytes.

Structural investigations of the formed complexes by EXAFS spectroscopy show a change of the coordination mode of lactate towards the NpO_2^+ center when varying the pH_c . With increasing pH_c the distance of the C-atom shell increases indicating a change of the coordination mode from end-on to side-on. Quantum chemical calculations confirm the bond distances determined by EXAFS for end-on and side-on coordination. Theoretical approximations of the Gibbs free energies for the isomerisation of end-on into side-on coordinated ligands show the preference of the end-on coordination for $\text{NpO}_2(\text{Lac})$ and of the side-on mode for $\text{NpO}_2(\text{Lac})_2^-$. However, effects of the proton concentration are not considered in the quantum chemical calculations, but the results agree with the trends observed by EXAFS as a function of the pH_c . In contrast to the EXAFS results, the ATR-FT infrared spectra show no effect of the proton concentration on the coordination mode but indicate a side-on coordination of lactate for $\text{pD}_c > 2.6$.

It is expected that different coordination modes of lactate have a strong impact on the thermodynamic functions ($\log \beta_n^0(T)$, $\Delta_r H_{n,m}^0$, $\Delta_r S_{n,m}^0$) of the NpO_2^+ complexes. Thus, for the determination of thermodynamic functions detailed information on the structure of the complexes and the coordination mode of the ligand are essential. In the present work the absorption spectroscopic studies were performed at $\text{pH}_c = 4.9$. At this pH_c lactate coordinates in the side-on mode forming chelate complexes. The present work is a detailed study on the complexation of NpO_2^+ with lactate providing thermodynamic data and structural information on the formed complexes. The results highlight the effect of the α -hydroxy group on the thermodynamic functions compared to simple monocarboxylates and the effect of the proton concentration on the coordination mode. Furthermore, the here determined data contribute to the thermodynamic database of actinides improving the scientific basis for understanding the chemical behaviour of pentavalent actinides in the presence of multifunctional organic ligands in aqueous solution.

5 Acknowledgements

The absorption spectroscopic measurements were carried out at the Institute for Nuclear Waste Disposal (INE) at Karlsruhe Institute of Technology (KIT). Dr. D. Fellhauer and Dr. M. Altmaier are acknowledged for providing the ^{237}Np and comprehensive experimental support. The KIT Institute for Beam Physics and Technology (IBPT) is acknowledged for the operation of the storage ring, the Karlsruhe Research Accelerator (KARA), and provision of beamtime at the KIT light source. The ATR-FT-IR measurements were performed at the Institute of Resource Ecology at the Helmholtz-Zentrum Dresden-Rossendorf (HZDR).

This work is supported by the German Federal Ministry for Economic Affairs and Energy (BMWi) under contract O2E11415H and the German Federal Ministry of Education and Research (BMBF) under contract O2NUK039C.

Literature

1. Gens, R.; Lalieux, P.; Preter, P. D.; Dierckx, A.; Bel, J.; Boyazis, J.-P.; Cool, W., The Second Safety Assessment and Feasibility Interim Report (SAFIR 2 Report) on HLW Disposal in Boom Clay: Overview of the Belgian Programme. *MRS Proceedings* **2011**, *807*, 917-924.
2. Oecd, N. E. A. *Safety of Geological Disposal of High-level and Long-lived Radioactive Waste in France* NUCLEAR ENERGY AGENCY ORGANISATION FOR ECONOMIC CO-OPERATION AND DEVELOPMENT: 2006.
3. Hoth, P.; Wirth, H.; Reinhold, K.; Bräuer, V.; Krull, P.; Feldrappe, H., Endlagerung radioaktiver Abfälle in tiefen geologischen Formationen Deutschlands–Untersuchung und Bewertung von Tongesteinsformationen. *BGR Bundesanstalt für Geowissenschaften und Rohstoffe, Hannover/Germany* **2007**.
4. NAGRA Projekt Opalinuston – Synthese der geowissenschaftlichen Untersuchungsergebnisse, Entsorgungsnachweis für abgebrannte Brennelemente, verglaste hochaktive sowie langlebige mittelaktive Abfälle; NAGRA Nationale Genossenschaft für die Lagerung radioaktiver Abfälle: Wettingen/Switzerland, 2002.
5. Mengel, K.; Röhlig, K.-J.; Geckeis, H., Endlagerung radioaktiver Abfälle. *Chem. unserer Zeit* **2012**, *46* (4), 208-217.
6. Geckeis, H.; Lutzenkirchen, J.; Polly, R.; Rabung, T.; Schmidt, M., Mineral-water interface reactions of actinides. *Chem. Rev.* **2013**, *113* (2), 1016-62.
7. Gaucher, E.; Robelin, C.; Matray, J. M.; Negral, G.; Gros, Y.; Heitz, J. F.; Vinsot, A.; Rebours, H.; Cassagnabere, A.; Bouchet, A., ANDRA underground research laboratory: interpretation of the mineralogical and geochemical data acquired in the Callovian-Oxfordian formation by investigative drilling. *Phys Chem Earth* **2004**, *29* (1), 55-77.
8. Allen, T. R.; Stoller, R. E.; Yamanaka, S., *Comprehensive Nuclear Materials*. Elsevier: Radarweg 29, PO Box 211, 1000 AE Amsterdam, The Netherlands, 2012.
9. Courdouan, A.; Christl, I.; Meylan, S.; Wersin, P.; Kretzschmar, R., Isolation and characterization of dissolved organic matter from the Callovo–Oxfordian formation. *Appl. Geochem.* **2007**, *22* (7), 1537-1548.
10. Courdouan, A.; Christl, I.; Meylan, S.; Wersin, P.; Kretzschmar, R., Characterization of dissolved organic matter in anoxic rock extracts and in situ pore water of the Opalinus Clay. *Appl. Geochem.* **2007**, *22* (12), 2926-2939.
11. Guillaumont, R.; Fanghänel, T.; Neck, V.; Fuger, J.; Palmer, D. A., *Update on the Chemical Thermodynamics of Uranium, Neptunium, Plutonium, Americium and Technetium*. Elsevier B.V.: 2003.
12. Lemire, R. J., *Chemical thermodynamics of neptunium and plutonium*. Elsevier: 2001; Vol. 4.
13. Hummel, W.; Anderegg, G.; Rao, L.; Puigdomenech, I.; Tochiyama, O., *Chemical Thermodynamics of Compounds and Complexes of U, Np, Pu, Am, Tc, Se, Ni and Zr with Selected Organic Ligands*. Elsevier B.V.: 2005.
14. Choppin, G. R., Actinide speciation in aquatic systems. *Mar. Chem.* **2006**, *99* (1-4), 83-92.
15. Choppin, G. R., Actinide speciation in the environment. *J. Radioanal. Nucl. Chem.* **2007**, *273* (3), 695-703.
16. Fanghänel, T.; Neck, V., Aquatic chemistry and solubility phenomena of actinide oxides/hydroxides. *Pure Appl. Chem.* **2002**, *74* (10), 1895-1907.
17. Maher, K.; Bargar, J. R.; Brown, G. E., Jr., Environmental speciation of actinides. *Inorg. Chem.* **2013**, *52* (7), 3510-32.
18. Moore, R. C.; Borkowski, M.; Bronikowski, M. G.; Chen, J.; Pokrovsky, O. S.; Xia, Y.; Choppin, G. R., Thermodynamic Modeling of Actinide Complexation with Acetate and Lactate at High Ionic Strength. *J. Solution Chem.* **1999**, *28* (5), 521-531.
19. Inoue, Y.; Tochiyama, O., Study of the complexes of Np(V) with organic ligands by solvent extraction with TTA and 1, 10-phenanthroline. *Polyhedron* **1983**, *2* (7), 627-630.

20. Vasiliev, A. N.; Banik, N. L.; Marsac, R.; Kalmykov, S. N.; Marquardt, C. M., Determination of complex formation constants of neptunium(V) with propionate and lactate in 0.5–2.6 m NaCl solutions at 22–60°C using a solvent extraction technique. *Radiochimica Acta* **2019**, *107* (7), 623-634.
21. Fellhauer, D.; Rothe, J.; Altmaier, M.; Neck, V.; Runke, J.; Wiss, T.; Fanghänel, T., Np(V) solubility, speciation and solid phase formation in alkaline CaCl₂ solutions. Part I: Experimental results. *Radiochimica Acta* **2016**, *104* (6), 355-379.
22. Müller, K.; Foerstendorf, H.; Brendler, V.; Bernhard, G., Sorption of Np(V) onto TiO₂, SiO₂, and ZnO: An *in situ* ATR FT-IR spectroscopic study. *Environ. Sci. Technol.* **2009**, *43* (20), 7665-7670.
23. Glasoe, P. K.; Long, F. A., Use of glass electrodes to measure acidities in deuterium oxide. *J. Phys. Chem.* **1960**, *64* (1), 188-190.
24. George, G. N.; Pickering, I. J., EXAFSPAK: A suite of computer programs for analysis of X-ray absorption spectra. *SSRL, Stanford* **1995**.
25. Ravel, B.; Newville, M., ATHENA, ARTEMIS, HEPHAESTUS: data analysis for X-ray absorption spectroscopy using IFEFFIT. *J Synchrotron Radiat* **2005**, *12* (Pt 4), 537-41.
26. Newville, M., IFEFFIT: interactive XAFS analysis andFEFFfitting. *Journal of Synchrotron Radiation* **2001**, *8* (2), 322-324.
27. Rehr, J. J.; Kas, J. J.; Prange, M. P.; Sorini, A. P.; Takimoto, Y.; Vila, F., Ab initio theory and calculations of X-ray spectra. *Comptes Rendus Physique* **2009**, *10* (6), 548-559.
28. Akhmerkina, Z. V.; Serezhkina, L. B.; Serezhkin, V. N.; Mikhajlov, Y. N.; Gorbunova, Y. E., Crystal structure of Ba[UO₂(C₂O₄)₂(H₂O)]·4H₂O. *Zhurnal Neorganicheskoy Khimii* **2004**, *49* (10), 1692-1695.
29. Lermontov, A. S.; Lermontova, E. K.; Wang, Y.-Y., Synthesis, structure and optic properties of 2-methylimidazolium and 2-phenylimidazolium uranyl acetates. *Inorg. Chim. Acta* **2009**, *362* (10), 3751-3755.
30. Furche, F.; Ahlrichs, R.; Hättig, C.; Klopper, W.; Sierka, M.; Weigend, F., Turbomole. *Wiley Interdisciplinary Reviews: Computational Molecular Science* **2014**, *4* (2), 91-100.
31. Becke, A. D., A new mixing of Hartree–Fock and local density-functional theories. *The Journal of Chemical Physics* **1993**, *98* (2), 1372.
32. Küchle, W.; Dolg, M.; Stoll, H.; Preuss, H., Energy-adjusted pseudopotentials for the actinides. Parameter sets and test calculations for thorium and thorium monoxide. *The Journal of Chemical Physics* **1994**, *100* (10), 7535.
33. Weigend, F.; Häser, M., RI-MP2: first derivatives and global consistency. *Theor. Chem. Acc.* **1997**, *97* (1-4), 331-340.
34. Weigend, F.; Häser, M.; Patzelt, H.; Ahlrichs, R., RI-MP2: optimized auxiliary basis sets and demonstration of efficiency. *Chemical Physics Letters* **1998**, *294* (1-3), 143-152.
35. Klamt, A.; Schüürmann, G., COSMO: a new approach to dielectric screening in solvents with explicit expressions for the screening energy and its gradient. *Journal of the Chemical Society, Perkin Transactions 2* **1993**, (5), 799.
36. Yang, Y.; Zhang, Z.; Liu, G.; Luo, S.; Rao, L., Effect of temperature on the complexation of NpO₂ + with benzoic acid: Spectrophotometric and calorimetric studies. *The Journal of Chemical Thermodynamics* **2015**, *80*, 73-78.
37. Zhang, Z.; Yang, Y.; Liu, G.; Luo, S.; Rao, L., Effect of temperature on the thermodynamic and spectroscopic properties of Np(v) complexes with picolinate. *RSC Advances* **2015**, *5* (92), 75483-75490.
38. Maiwald, M. M.; Skerencak-Frech, A.; Panak, P. J., The complexation and thermodynamics of neptunium(V) with acetate in aqueous solution. *New J. Chem.* **2018**, *42* (10), 7796-7802.
39. Maiwald, M. M.; Sittel, T.; Fellhauer, D.; Skerencak-Frech, A.; Panak, P. J., Thermodynamics of neptunium(V) complexation with sulfate in aqueous solution. *The Journal of Chemical Thermodynamics* **2018**, *116*, 309-315.
40. Maiwald, M. M.; Fellhauer, D.; Skerencak-Frech, A.; Panak, P. J., The complexation of neptunium(V) with fluoride at elevated temperatures: Speciation and thermodynamics. *Appl. Geochem.* **2019**, *104*, 10-18.
41. Neck, V.; Fanghänel, T.; Rudolph, G.; Kim, J. I., Thermodynamics of Neptunium(V) in Concentrated Salt Solutions: Chloride Complexation and Ion Interaction (Pitzer) Parameters for the NpO₂ + Ion. *Radiochimica Acta* **1995**, *69* (1), 39-47.

42. Skerencak, A.; Panak, P. J.; Hauser, W.; Neck, V.; Klenze, R.; Lindqvist-Reis, P.; Fanghänel, T., TRLFS study on the complexation of Cm(III) with nitrate in the temperature range from 5 to 200 degrees C. *Radiochimica Acta* **2009**, *97* (8), 385-393.
43. Skerencak, A.; Panak, P. J.; Fanghänel, T., Complexation and thermodynamics of Cm(III) at high temperatures: the formation of $[Cm(SO_4)_n]^{3-2n}$ ($n = 1, 2, 3$) complexes at $T = 25$ to $200^\circ C$. *Dalton Trans.* **2013**, *42*, 542-549.
44. Fröhlich, D. R.; Skerencak-Frech, A.; Kaplan, U.; Koke, C.; Rossberg, A.; Panak, P. J., An EXAFS spectroscopic study of Am(III) complexation with lactate. *J Synchrotron Radiat* **2015**, *22* (6), 1469-74.
45. Skerencak-Frech, A.; Taube, F.; Zanonato, P. L.; Acker, M.; Panak, P. J.; Di Bernardo, P., A potentiometric and microcalorimetric study of the complexation of trivalent europium with lactate: The ionic strength dependency of $\log \beta'_n$, $\Delta rH_{m,n}$ and $\Delta rS_{m,n}$. *Thermochim. Acta* **2019**, 679.
46. Fröhlich, D. R.; Skerencak-Frech, A.; Panak, P. J., A spectroscopic study on the formation of Cm(III) acetate complexes at elevated temperatures. *Dalton Trans* **2014**, *43* (10), 3958-65.
47. Zalupski, P. R.; Nash, K. L.; Martin, L. R., Thermodynamic Features of the Complexation of Neodymium(III) and Americium(III) by Lactate in Trifluoromethanesulfonate Media. *J. Solution Chem.* **2010**, *39*, 1213-1229.
48. Nilsson, M.; Nash, K. L., Trans-Lanthanide Extraction Studies in the TALSPEAK System: Investigating the Effect of Acidity and Temperature. *Solvent Extr. Ion Exch.* **2009**, *27* (3), 354-377.
49. Martell, A. E. a. S., R.M. and Motekaitis, R.J., *NIST standard reference database 46 version 8.0: NIST critically selected stability constants of metal complexes*. U.S. Department of Commerce, Technology Administration, National Institute of Standards and Technology, Standard Reference Data Program: Gaithersburg, MD, 2004.
50. Lemire, R.; Berner, U.; Musikas, C.; Palmer, D.; Taylor, P.; Tochiyama, O., Chemical thermodynamics of iron. *Nuclear Energy Agency, OECD, Elsevier* **2013**.
51. Skerencak-Frech, A.; Maiwald, M.; Trumm, M.; Fröhlich, D. R.; Panak, P. J., The complexation of Cm(III) with oxalate in aqueous solution at $T = 20-90$ degrees C: a combined TRLFS and quantum chemical study. *Inorg. Chem.* **2015**, *54* (4), 1860-8.
52. Skerencak, A.; Panak, P. J.; Neck, V.; Trumm, M.; Schimmelpfennig, B.; Lindqvist-Reis, P.; Klenze, R.; Fanghänel, T., Complexation of Cm(III) with fluoride in aqueous solution in the temperature range from 20 to 90 degrees C. A joint TRLFS and quantum chemical study. *J. Phys. Chem. B* **2010**, *114* (47), 15626-34.
53. Inoue, Y.; Tochiyama, O.; Takahashi, T., Study of the Carboxylate Complexing of Np(V) by Solvent Extraction with TTA and Capriquat. *Radiochimica Acta* **1982**, *31* (3-4).
54. Vasiliev, A. N.; Banik, N. L.; Marsac, R.; Fröhlich, D. R.; Rothe, J.; Kalmykov, S. N.; Marquardt, C. M., Np(v) complexation with propionate in 0.5-4 M NaCl solutions at 20-85 degrees C. *Dalton Trans* **2015**, *44* (8), 3837-44.
55. Maiwald, M. M.; Dardenne, K.; Rothe, J.; Skerencak-Frech, A.; Panak, P. J., Thermodynamics and Structure of Neptunium(V) Complexes with Formate. Spectroscopic and Theoretical Study. *Inorg. Chem.* **2020**.
56. Allen, P. G.; Bucher, J. J.; Shuh, D. K.; Edelstein, N. M.; Reich, T., Investigation of Aquo and Chloro Complexes of UO_2^{2+} , NpO_2^{2+} , Np^{4+} , and Pu^{3+} by X-ray Absorption Fine Structure Spectroscopy. *Inorg. Chem.* **1997**, *36* (21), 4676-4683.
57. Reich, T.; Bernhard, G.; Geipel, G.; Funke, H.; Hennig, C.; Roßberg, A.; Matz, W.; Schell, N.; Nitsche, H., The Rossendorf Beam Line ROBL – a dedicated experimental station for XAFS measurements of actinides and other radionuclides. *Radiochimica Acta* **2000**, *88* (9-11).
58. Takao, K.; Takao, S.; Scheinost, A. C.; Bernhard, G.; Hennig, C., Complex formation and molecular structure of neptunyl(VI) and -(V) acetates. *Inorg. Chem.* **2009**, *48* (18), 8803-10.
59. Fröhlich, D. R.; Skerencak-Frech, A.; Bauer, N.; Rossberg, A.; Panak, P. J., The pH dependence of Am(III) complexation with acetate: an EXAFS study. *J Synchrotron Radiat* **2015**, *22* (1), 99-104.
60. Cassanas, G.; Morsli, M.; Fabregue, E.; Bardet, L., Vibrational-spectra of lactic-acid and lactates. *Journal of Raman Spectroscopy* **1991**, *22* (7), 409-413.
61. Hesse, M.; Meier, H.; Zeeh, B., *Spektroskopische Methoden in der organischen Chemie*. 7. Auflage ed.; Georg Thieme Verlag: 2005.

62. Jones, L. H.; Penneman, R. A., Infrared Spectra and Structure of Uranyl and Transuranium(V) and(VI) Ions in Aqueous Perchloric Acid Solution. *J. Chem. Phys.* **1953**, *21* (3), 542-544.
63. Deacon, G. B.; Phillips, R. J., Relationships between the carbon-oxygen stretching frequencies of carboxylato complexes and the type of carboxylate coordination. *Coord. Chem. Rev.* **1980**, *33* (3), 227-250.
64. Kakihana, M.; Nagumo, T.; Okamoto, M.; Kakihana, H., Coordination structures for uranyl carboxylate complexes in aqueous-solution studied by IR and C-13 NMR-Spectra. *J. Phys. Chem.* **1987**, *91* (24), 6128-6136.